Nonlinear behavior of planar compliant tensegrity mechanism with variable free-lengths

Tyler Rhodes[1], Miranda Tanouye[1], and Vishesh Vikas[1]

[1]Agile Robotics Lab,
University of Alabama, Tuscaloosa AL USA
Email: {trhodes1,mtanouye}@crimson.ua.edu, vvikas@ua.edu

Abstract

Traditional tensegrity mechanisms comprise compressive (rigid rods) and tensile members (cables). Compliant tensegrity mechanisms (CoTM) include springs alongside cables. Introduction of spring elements allows these structures to be more adaptable and robust. The kinematic and stability analyses of such mechanisms will facilitate better understanding of their behaviors for developing control and design methodologies. The analysis of CoTM often involves making the zero free-length (ZFL) assumption, i.e., the free-length of the spring is zero, which disqualifies the analysis for most real-word applications. The paper illustrates the drastic increase in computational complexity for finding static solutions as the assumption of ZFL for spring elements are relaxed for a simple planar compliant tensegrity mechanism comprising of two rigid triangular platforms connected by a compressive member and two spring elements. The resulting non-linear behavior of obtained static solutions shows intersecting manifolds of equilibrium orientation angles where the number of solutions vary from minimum of 4 to beyond 10 as the spring free-lengths are varied.

Keywords: tensegrity, compliant mechanisms, non-zero free-length

1 Introduction

Tensegrity mechanisms are made up of compressive and tensile members where no pair of struts touch and each end is connected to three non-coplanar ties. This provides some unique features: strain is distributed through deformation of the structure, they expand in all axes at once, and can be built from one another [1]. These unique properties render them useful in the fields of robotics [2, 3], space applications [4], bridges [5] and biological modeling [6]. Several natural structures can be modeled as a tensegrity, such as the human spine [7] and DNA supermolecules [8]. Their ability to withstand large amounts of strain and effi-

cient packing (occupying less volume for storage) make them ideal for deployment applications [9].

Static analysis, dynamic and stability analysis of traditional tensegrity mechanism provide insight into their behavior [10–14]. The direct static problem yields equilibrium equations which are nonlinear in the angle, thus, yielding multiple equilibrium solutions. The analytical solution structure of the equilibrium equations is of special interest as they are helpful in providing the bound on the number of possible solutions. Some analytical solutions for prestressed tensegrity structures have been proposed and explored [15, 16].

Compliant Tensegrity Mechanisms (CoTM) augment traditional tensegrity structures by adding springs elements that can compress and as well as extend. Moreover, the mechanism orientation may be controlled through its compliance, such as by indirectly varying free lengths of the spring elements. Such modifications have been experimentally introduced to build tensegrity robots, however, their kinematic analysis has been limited [17,18]. The presented research analyzes the effect of variation of spring free lengths on the static equilibrium and stability of a planar tensegrity mechanism.

Commonly, the static and dynamic analysis of these structures assumes zero free-lengths (ZFL). For a ZFL spring, the unstretched (free) length of a linear spring is zero and a general ZFL spring is not an existing product [19], however, can be realized through different methodologies including pretension [20] and geometric manipulation [21]. This ZFL assumption greatly simplifies the analysis of the system but is difficult to implement in practice. The paper presents detailed analysis for an example planar CoTM where ZFL assumption is gradually relaxed 1) both springs have ZFL, 2) one spring has ZFL and 3) no springs have ZFLs. The application of the presented analysis will be instrumental in control, modeling of deployable CoTM structures, and tensegrity based biomechanical modeling.

2 Problem Statement and Definition

The proposed mechanism consists of two triangular rigid bodies connected by a rigid rod and two springs members as shown in Figure (1) where the relative distance between points $1, 4$ is L_3. The spring free lengths and spring constants are denoted by L_{0i}, k_i where $i = 1, 2$. The objective is to find all of its stable equilibrium positions, as defined by γ_1 and γ_2, for a given set of parameters.

As illustrated in Figure (1), let the coordinate system B be fixed on the bottom rigid body with origin at point 1, x-axis between points 1, 2 and z-axis out of the plane of paper. Similarly, the coordinate system T is fixed on the top rigid body with origin at point 4, x-axis between points 4, 6 and z-axis out of the plane of paper. Let ${}^A\boldsymbol{P}_i, \boldsymbol{P}_{i\to j}$ represent a point i in coordinate system A and vector between points i and j respectively. Consequently, the points are

$$ {}^B\boldsymbol{P}_2 = [p_{2x}, 0, 0]^T \quad , \quad {}^B\boldsymbol{P}_3 = [p_{3x}, p_{3y}, 0]^T \tag{1} $$

$$ {}^T\boldsymbol{P}_5 = [p_{5x}, 0, 0]^T \quad , \quad {}^T\boldsymbol{P}_6 = [p_{6x}, p_{6y}, 0]^T \tag{2} $$

The transformation matrix ${}^{T}_{B}\boldsymbol{T}$ between coordinate system T and B is written as

$$ {}^{T}_{B}\boldsymbol{T} = \begin{bmatrix} c_2 & -s_2 & 0 & L_3 c_1 \\ s_2 & c_2 & 0 & L_3 s_1 \\ 0 & 0 & 1 & 0 \\ 0 & 0 & 0 & 1 \end{bmatrix} \tag{3} $$

where c_i, s_i are $\cos\gamma_i, \sin\gamma_i$ corresponding to angles γ_1, γ_2 shown in Figure 1. Hence, for $i = 4, 5$

$$ \begin{bmatrix} {}^{B}\boldsymbol{P}_i \\ 1 \end{bmatrix} = {}^{T}_{B}\boldsymbol{T} \begin{bmatrix} {}^{T}\boldsymbol{P}_i \\ 1 \end{bmatrix} \tag{4} $$

The superscript will be dropped for remaining section of the paper as all the calculations will be performed in the B coordinate system. Let f_3 be the unknown force along the rigid bar and $d_i, f_i = k_i(d_i - L_{0i})\ \forall i = 1, 2$ be the length and forces in spring elements. Using screw theory notation, for static equilibrium, sum of the three wrenches along the corresponding tensegrity elements is zero

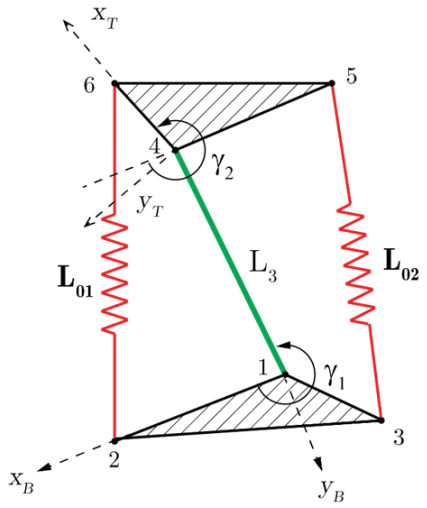

Figure 1: The proposed planar Compliant Tensegrity Mechanism (CoTM) comprises of two triangular rigid bodies connected by a rigid rod (green) and two spring members (red).

$$ \frac{f_1}{d_1} \begin{bmatrix} \boldsymbol{P}_{2\to6} \\ \boldsymbol{P}_{2\to6} \times \boldsymbol{P}_{1\to2} \end{bmatrix} + \frac{f_2}{d_2} \begin{bmatrix} \boldsymbol{P}_{3\to5} \\ \boldsymbol{P}_{3\to5} \times \boldsymbol{P}_{1\to3} \end{bmatrix} + f_3 \begin{bmatrix} \boldsymbol{P}_{1\to4} \\ 0 \end{bmatrix} = 0 \tag{5} $$

The analysis results in four equations of interest - two equilibrium equations coupled with two constraint equations

$$ k_1 \left(1 - \frac{L_{01}}{d_1}\right) (\boldsymbol{P}_{2\to6} \times \boldsymbol{P}_{1\to4}) + k_2 \left(1 - \frac{L_{02}}{d_2}\right) (\boldsymbol{P}_{3\to5} \times \boldsymbol{P}_{1\to4}) = 0 \tag{6a} $$

$$ k_1 \left(1 - \frac{L_{01}}{d_1}\right) (\boldsymbol{P}_{2\to6} \times \boldsymbol{P}_{1\to2}) + k_2 \left(1 - \frac{L_{02}}{d_2}\right) (\boldsymbol{P}_{3\to5} \times \boldsymbol{P}_{1\to3}) = 0 \tag{6b} $$

$$ d_1^2 - \|\boldsymbol{P}_{2\to6}\|^2 = 0 \tag{7a} $$

$$ d_2^2 - \|\boldsymbol{P}_{3\to5}\|^2 = 0 \tag{7b} $$

3 Equilibrium and Stability Analysis

3.1 Case 1: Both Springs are have Zero Free-Length

Equilibrium Analysis. For the first case, both springs are assumed to have ZFL i.e. $L_{01} = L_{02} = 0$. The variables d_1 and d_2 do not appear in the equilibrium

equations as a result of ZFL assumption, hence, Equations (6a),(6b) are decoupled from Equations (7a),(7b). However, these equations are non-linear in the desired equilibrium angles with constrained solution space $c_i, s_i \in [-1, 1]\ \forall i = 1, 2$. Tan-half angle identities are instrumental in converting these equations to polynomial form with unconstrained solution space where $x_i \in [-\infty, \infty]$

$$c_i = \frac{1 - x_i^2}{1 + x_i^2}, s_i = \frac{2x_i}{1 + x_i^2} \quad \text{where} \quad x_i = \tan\frac{\gamma_i}{2} \forall i = 1, 2 \tag{8}$$

The resulting polynomial form of Equations (6a),(6b) is

$$f_1(x_1, x_2) = C_1(x_2)x_1^2 + C_2(x_2)x_1 + C_3(x_2) = 0 \tag{9a}$$

$$f_2(x_1, x_2) = D_1(x_2)x_1^2 + D_2(x_2)x_1 + D_3(x_2) = 0 \tag{9b}$$

where the coefficients $C_i(x_2), D_i(x_2) \forall i = 1, 2, 3$ are second order polynomials in x_2 and are listed in Appendix (A). The solution of this system of equations can be obtained through polynomial elimination by constructing a Sylvester matrix [22, 23]. The coefficients for x_1 in Equations (9a),(9b) are combined to create a linear system of the form

$$\begin{bmatrix} C_1 & C_2 & C_3 & 0 \\ 0 & C_1 & C_2 & C_3 \\ D_1 & D_2 & D_3 & 0 \\ 0 & D_1 & D_2 & D_3 \end{bmatrix} \begin{bmatrix} x_1^3 \\ x_1^2 \\ x_1 \\ 1 \end{bmatrix} = \begin{bmatrix} 0 \\ 0 \\ 0 \\ 0 \end{bmatrix} \tag{10}$$

As these system of equations have a non-trivial solution, the determinant of the 4×4 Sylvester matrix needs to be zero. This determinant will result in a sixth (6) degree polynomial in variable x_2 which can be numerically solved.

Uniqueness. There is a one-to-one mapping between x_1 and x_2 i.e. for a given solution of x_2, there exists a unique x_1. The unique x_1 can be calculated by rearranging Equation (10) and substituting x_2 into the coefficients.

$$\begin{bmatrix} x_1^3 \\ x_1^2 \\ x_1 \end{bmatrix} = \begin{bmatrix} C_1(x_2) & C_2(x_2) & C_3(x_2) \\ 0 & C_1(x_2) & C_2(x_2) \\ D_1(x_2) & D_2(x_2) & D_3(x_2) \end{bmatrix}^{-1} \begin{bmatrix} 0 \\ -C_3(x_2) \\ 0 \end{bmatrix} \tag{11}$$

As evident from Equation (8), x_1 and x_2 correspond to unique γ_1 and γ_2.

Stability Analysis. The interest of this study is not only evaluating all possible solutions of a given system, but determining the stability of these solutions by observing the eigenvalues of the Jacobian $\boldsymbol{J}_{L_{01}=0, L_{02}=0}$. The Jacobian was constructed from the force and torque equations with respect to the dependent variables x_1 and x_2

$$\boldsymbol{J}_{L_{01}=0, L_{02}=0} = \begin{bmatrix} f_{1,x_1} & f_{1,x_2} \\ f_{2,x_1} & f_{2,x_2} \end{bmatrix} \tag{12}$$

where $f_{i,x} = \dfrac{\partial f_i}{\partial x}$. The corresponding solution is described as stable if the real parts of all the eigenvalues are negative.

3.2 Case 2: One spring has Zero Free-Length

Equilibrium Analysis. For the scenario when only one of the springs is assumed to have ZFL i.e. $L_{01} \neq 0, L_{02} = 0$, the equilibrium Equations (7a),(7b) are coupled with the constraint Equation (6a) through a third variable d_1. Polynomial conversion results in

$$g_1(x_1, x_2, d_1) = (E_{1,1}d_1 + E_{1,2})x_1^2 + (E_{2,1}d_1 + E_{2,2})x_1 + (E_{3,1}d_1 + E_{3,2}) \quad (13a)$$

$$g_2(x_1, x_2, d_1) = (F_{1,1}d_1 + F_{1,2})x_1^2 + (F_{2,1}d_1 + F_{2,2})x_1 + (F_{3,1}d_1 + F_{3,2}) \quad (13b)$$

$$g_3(x_1, x_2, d_1) = \left[(1 + x_2^2)\right](1 + x_1^2)d_1^2 - (G_1x_1^2 + G_2x_1 + G_3) \quad (13c)$$

where $E_{i,j}(x_2)$, $F_{i,j}(x_2)$ and $G_{i,j}(x_2)$ coefficients are listed in Appendix (B). The system is reduced to two equations in variables x_1, x_2 by substituting for the linear solution of d_1 from Equations (13a),(13b) into Equation (13c).

$$g_4(x_1, x_2) = J_6x_1^6 + J_5x_1^5 + J_4x_1^4 + J_3x_1^3 + J_2x_1^2 + J_1x_1 + J_0 \quad (14a)$$

$$g_5(x_2, x_2) = K_6x_1^6 + K_5x_1^5 + K_4x_1^4 + K_3x_1^3 + K_2x_1^2 + K_1x_1 + K_0 \quad (14b)$$

where J_i and K_i are 6th degree polynomials in x_2. The resulting 12×12 Sylvester matrix is formulated similar to Equation (10) and is dependent only on x_2. The determinant of this matrix results in a 72-degree polynomial in x_2.

Uniqueness. It is easy to observe that for a given solution of x_2, unique $x_1, d_1, \gamma_1, \gamma_2$ can be obtained by rearranging the Sylvester matrix and Equations (13c),(8).

Stability Analysis. The Jacobian $\boldsymbol{J}_{L_{01}\neq 0, L_{02}=0}$ is constructed using Equations (13a)-(13c) and the system is termed stable when the real part of all the eigenvalue are negative.

$$\boldsymbol{J}_{L_{01}\neq 0, L_{02}=0} = \begin{bmatrix} g_{1,x_1} & g_{1,x_2} & g_{1,d_1} \\ g_{2,x_1} & g_{2,x_2} & g_{2,d_1} \\ g_{3,x_1} & g_{3,x_2} & g_{3,d_1} \end{bmatrix} \quad (15)$$

3.3 Case 3: None of the springs have Zero Free-Lengths

Equilibrium Analysis. When the ZFL constraint for both the springs are relaxed, the complexity increases even further as the equilibrium and both constraint equations are coupled through variables d_1, d_2.

$$h_1(x_1, x_2, d_1, d_2) = L_1x_1^2 + L_2x_1 + L_3 \quad (16a)$$

$$h_2(x_1, x_2, d_1, d_2) = M_1x_1^2 + M_2x_1 + M_3 \quad (16b)$$

$$h_3(x_1, x_2, d_1, d_2) = (1 + x_1^2)(1 + x_2^2)d_1^2 - (N_1x_1^2 + N_2x_1 + N_3) \quad (16c)$$

$$h_4(x_1, x_2, d_1, d_2) = (1 + x_1^2)(1 + x_2^2)d_2^2 - (O_1x_1^2 + O_2x_1 + O_3) \quad (16d)$$

The coefficients $L_i(x_2, d_1, d_2)$, $M_i(x_2, d_1, d_2)$, $N_i(x_2)$, $O_i(x_2) \forall i = 1, 2, 3$ are listed in Appendix (C). This scenario is presents computational challenge as the polynomial elimination algorithms become inefficient [22] but can be numerically approached using homotopy-based numerical techniques.

Stability Analysis. Again, the Jacobian $\boldsymbol{J}_{L_{01}\neq 0, L_{02}\neq 0}$ is constructed using Equations (16a)-(16d) and the system is stable when the real part of all the eigenvalues are negative.

$$\boldsymbol{J}_{L_{01}\neq 0, L_{02}\neq 0} = \begin{bmatrix} h_{1,x_1} & h_{1,x_2} & h_{1,d_1} & h_{1,d_2} \\ h_{2,x_1} & h_{2,x_2} & h_{2,d_1} & h_{2,d_2} \\ h_{3,x_1} & h_{3,x_2} & h_{3,d_1} & h_{3,d_2} \\ h_{4,x_1} & h_{4,x_2} & h_{4,d_1} & h_{4,d_2} \end{bmatrix} \tag{17}$$

4 Numerical Examples and Discussion

Case 1. For an example mechanisms with parameters as listed in Table (1) where both springs have ZFL, the roots of the sixth order polynomial resulting from polynomial elimination are tabulated in Table (2) where only the third solution is stable. The four real solutions are illustrated in Figure (2), with the stable solution in bold.

Table 1: CoTM parameters

Parameter	Value
L_3	9 m
k_1, k_2	$2.81N/m$
p_{2x}	$3.19m$
p_{3x}, p_{3y}	$-2.55, 4.93m$
p_{6x}	$4.25m$
p_{5x}, p_{5y}	$-0.3, -3.45m$

Table 2: Solutions for Case 1

Solution	γ_1 (deg)	γ_2 (deg)
1	75.034	289.04
2	276.53	330.79
3 (stable)	**252.35**	**123.74**
4	93.67	124.97
5,6	-149.80 $\pm i85.41$	-160.71 $\pm i167.38$

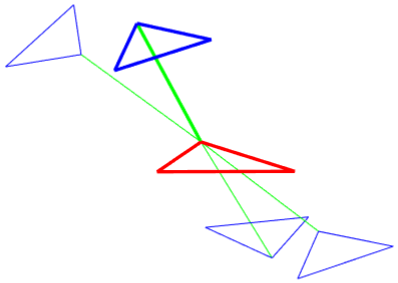

Figure 2: Visualization of solutions for when both springs have ZFL. The four real solutions are indicated where the fixed bottom rigid body, the top rigid body and the compressive rigid member are marked in red, blue and green respectively. The single stable solution is marked in bold.

Case 2: One spring has ZFL. The ZFL constraint was relaxed for the CoTM example with $L_{01} = 11.5m$. The analytical solution resulted in a 72-degree polynomial with 14 real solutions. These solutions are listed in Table (3) and illustrated in Figure (3) where the 8th, 12th and 14th solutions were stable. **Case 3:**

Table 3: Solutions for Case 2 where $L_{01} = 11.5m$. Stable solutions in bold.

	γ_1(deg)	γ_2(deg)	d_1(m)
1	121.69	−170.30	13.95
2	−53.70	−137.78	10.16
3	−134.63	−118.07	−15.35
4	109.42	−113.03	9.08
5	43.84	−111.10	−2.88
6	108.06	−79.05	6.78
7	115.19	−5.97	−8.19

	γ_1(deg)	γ_2(deg)	d_1(m)
8	**−49.06**	**13.59**	**−8.97**
9	121.04	41.45	11.50
10	−121.20	64.23	−7.14
11	−57.21	65.86	5.03
12	**35.41**	**67.86**	**−10.81**
13	−55.72	94.46	−3.56
14	**129.99**	**112.18**	**−15.14**

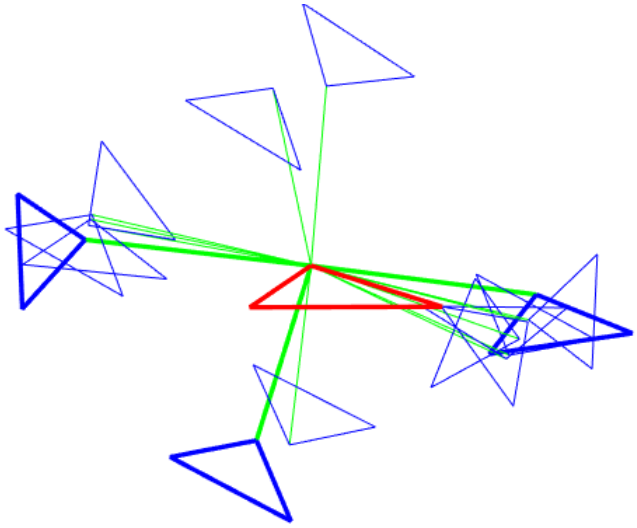

Figure 3: Fourteen real solutions were obtained when the ZFL assumption was relaxed for one spring element of which three were stable (marked in bold).

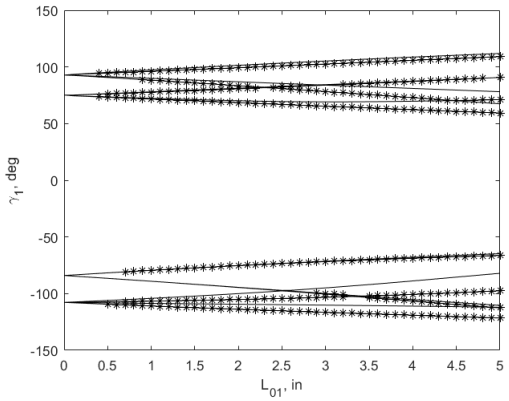

Figure 4: Solutions of γ_1 as L_{01} is varied with stable solutions marked with '*'.

No springs have ZFLs. Solving four polynomial equations in four becomes unfeasible for traditional polynomial elimination methods [22]. Bertini software [24] was used to numerically obtain 88 solutions for $L_{01} = L_{02} = 11.5m$. Thirty of these solutions were real of which five were found to be stable as collated' in Table (4) and Figure (5) respectively.

Table 4: Solutions for Case 3 ($L_{01} = L_{02} = 11.5m$). Stable ones are highlighted.

	γ_1(deg)	γ_2(deg)
1	118.75	35.52
2	1.86	11.31
3	123.69	48.35
4	158.85	147.91
5	27.01	−135.42
6	81.58	−60.61
7	114.38	24.21
8	113.32	148.87
9	158.45	−18.37
10	121.96	43.85
11	−16.11	152.17
12	1.55	−177.34
13	116.20	−141.81
14	**−99.16**	**157.70**
15	**−178.95**	**−69.89**

	γ_1(deg)	γ_2(deg)
16	−109.34	109.14
17	−60.03	49.95
18	−119.62	−94.00
19	−82.25	−172.07
20	−92.63	−46.78
21	−173.90	5.31
22	−1.03	−33.82
23	−59.06	−143.69
24	111.37	16.39
25	52.62	85.56
26	**56.10**	**108.90**
27	118.69	−152.47
28	**48.02**	**60.96**
29	**−60.20**	**−120.65**
30	113.25	21.29

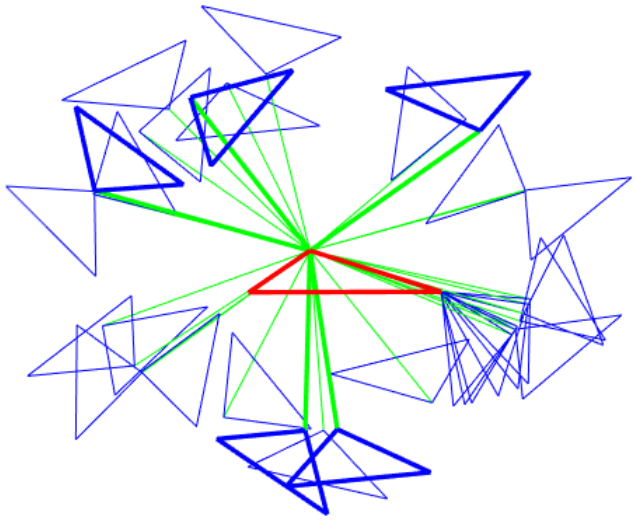

Figure 5: Example solutions when the ZFL assumptions are completely relaxed. Five stable solutions (bold) were observed out of the resulting thirty real solutions.

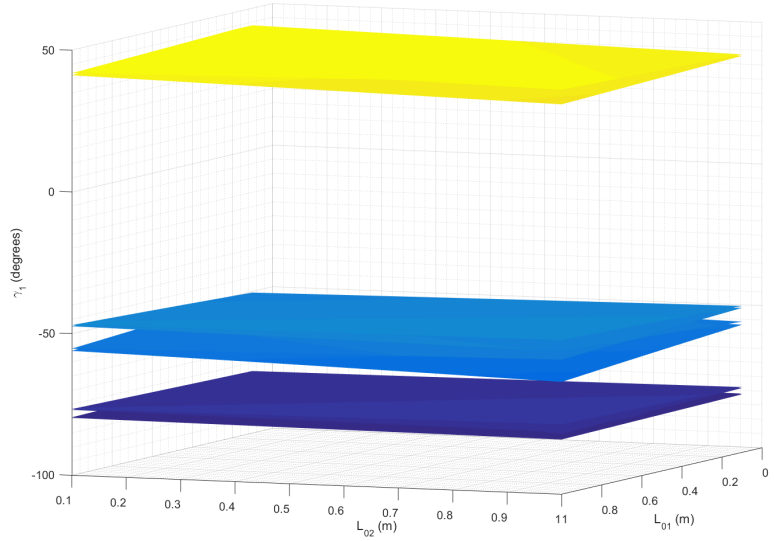

Figure 6: The intersecting solution manifolds for γ_2

Discussion

Complexity. As the ZFL assumption was relaxed, the overall computational complexity of this simple planar example increased exponentially such that the analytical solution could not be obtained in the third case. Moving forward to a 3D CoTM example is only expected to increase in complexity further. Finding better methods for solving these complex polynomials will be a continuous problem in this study. The Bertini software was used instead to solve for the solutions, as a result, the degree of the solution polynomial remains unknown and correspondingly, the total number of possible solutions.

Nonlinear behavior with change in free-length. The behavior of the mechanism as a function of free-lengths is of special interest due to possible applications in robust control of deployable structure and tensegrity-based biomechanical modeling. The Figure (4) shows the change in orientation of the mechanism (γ_1) as the free-length L_{01} is varied. The behavior of CoTM orientation is nonlinear - 4 real solutions for ZFL assumption bifurcate to as many as 10. This implies that it is possible to move from one orientation to another by slowly shortening or lengthening the free length of L_{01}, thus, controlling the mechanisms movement. This can be done by altering the length of the string on the cable-spring series combination of the tensile element of the mechanism. It also shows that as free length increases, the behavior of the system changes and the number of stable equilibrium solutions vary. The top set and bottom set of solutions are very simi-

lar in terms of pattern - this may imply that for some solutions there is a mirrored configuration. Stable solutions are marked with asterisk and start to appear when L_{01}=0.4 m and tend to follow one bifurcation line. Where these lines intersect, the system loses stability except for around $(4.5m, 77.35\,\text{deg})$ where the stable solutions start to follow the line they intersected with. The Figure (6) shows intersecting solution manifolds along which the mechanism can be maneuvered for obtaining robust, energy efficient control of the example mechanism.

CONCLUSION

This paper presented a method for determining the stable equilibrium solutions for a planar compliant tensegrity mechanism that is comprised of two rigid bodies connected by a compressive member and two spring members. Complexity of the problem increased dramatically from assuming a) both ZFL springs - sixth degree polynomial corresponding to equilibrium orientations; b) only one spring ZFL - 72-degree polynomial; c) no ZFL spring - 88 numerical solutions for example problem but unknown degree of polynomial using homotopy-based Bertini numerical software. The resulting behavior of the mechanism as ZFL assumption for one spring is relaxed and varied is also observed. Here, the stable solutions show how to control the configuration of the mechanism through compliance of the springs by shortening or lengthening its free length. This control is possible by varying L_{01} to move between desired γ_1 solutions.

Appendices

A Coefficients for Equations (9a),(9b)

$$C_i(x_2) = A_{i,2}x_2^2 + A_{i,1}x_2 + A_{i,0} \tag{18a}$$

$$D_i(x_2) = B_{i,2}x_2^2 + B_{i,1}x_2 + B_{i,0} \qquad \forall i = 1,2 \tag{18b}$$

$$A_{1,2} = L_3(k_2p_{3y} + k_2p_{5y}) \qquad B_{1,2} = L_3k_2p_{3y} - k_2p_{3x}p_{5y} + k_2p_{5x}p_{3y}$$

$$A_{1,1} = -L_3(2k_1p_{6x} + 2k_2p_{5x}) \qquad B_{1,1} = 2k_1p_{2x}p_{6x} + 2k_2p_{3x}p_{5x} + 2k_2p_{3y}p_{5y}$$

$$A_{1,0} = L_3(k_2p_{3y} - k_2p_{5y}) \qquad B_{1,0} = L_3k_2p_{3y} + k_2p_{3x}p_{5y} - k_2p_{5x}p_{3y}$$

$$A_{2,2} = L_3(2k_1p_{2x} + 2k_2p_{3x} + 2k_1p_{6x} + 2k_2p_{5x}) \qquad B_{2,2} = 2L_3k_1p_{2x} + 2L_3k_2p_{3x}$$

$$A_{2,1} = 4L_3k_2p_{5y} \qquad B_{2,1} = 0$$

$$A_{2,0} = L_3(2k_1p_{2x} + 2k_2p_{3x} - 2k_1p_{6x} - 2k_2p_{5x}) \qquad B_{2,0} = 2L_3k_1p_{2x} + 2L_3k_2p_{3x}$$

$$A_{3,2} = -L_3(k_2p_{3y} + k_2p_{5y}) \qquad B_{3,2} = k_2p_{5x}p_{3y} - k_2p_{3x}p_{5y} - L_3k_2p_{3y}$$

$$A_{3,1} = L_3(2k_1p_{6x} + 2k_2p_{5x}) \qquad B_{3,1} = 2k_1p_{2x}p_{6x} + 2k_2p_{3x}p_{5x} + 2k_2p_{3y}p_{5y}$$

$$A_{3,0} = -L_3(k_2p_{3y} - k_2p_{5y}) \qquad B_{3,0} = k_2p_{3x}p_{5y} - l_3k_2p_{3y} - k_2p_{5x}p_{3y}$$

B Coefficients for Equations (13a)-(13c)

$$
\begin{aligned}
E_1 =&(L_3(d_1k_2p_{3y} + d_1k_2p_{5y}))x_2^2 + (2L_3(L_{01}k_1p_{6x} - d_1k_1p_{6x} - d_1k_2p_{5x}))x_2 \\
&+ L_3(d_1k_2p_{3y} - d_1k_2p_{5y}) \\
E_2 =&(L_3(2d_1k_1p_{2x} - 2L_{01}k_1p_{6x} - 2L_{01}k_1p_{2x} + 2d_1k_2p_{3x} \\
&+ 2d_1k_1p_{6x} + 2d_1k_2p_{5x}))x_2^2 + (4L_3d_1k_2p_{5y})x_2 \\
&- L_3(2L_{01}k_1p_{2x} - 2L_{01}k_1p_{6x} - 2d_1k_1p_{2x} - 2d_1k_2p_{3x} \\
&+ 2d_1k_1p_{6x} + 2d_1k_2p_{5x}) \\
E_3 =&(-L_3(d_1k_2p_{3y} + d_1k_2p_{5y}))x_2^2 \\
&+ (L_3(2d_1k_1p_{6x} - 2L_{01}k_1p_{6x} + 2d_1k_2p_{5x}))x_2 \\
&- L_3(d_1k_2p_{3y} - d_1k_2p_{5y}) \\
F_1 =&d_1k_2(L_3p_{3y} - p_{3x}p_{5y} + p_{5x}p_{3y})x_2^2 \\
&+ (2d_1k_1p_{2x}p_{6x} + 2d_1k_2p_{3x}p_{5x} + 2d_1k_2p_{3y}p_{5y} \\
&- 2L_{01}k_1p_{2x}p_{6x})x_2 + d_1k_2(L_3p_{3y} + p_{3x}p_{5y} - p_{5x}p_{3y}) \\
F_2 =&2L_3(x_2^2 + 1)(d_1k_1p_{2x} - L_{01}k_1p_{2x} + d_1k_2p_{3x}) \\
F_3 =&- d_1k_2(L_3p_{3y} + p_{3x}p_{5y} - p_{5x}p_{3y})x_2^2 \\
&+ (2d_1k_1p_{2x}p_{6x} + 2d_1k_2p_{3x}p_{5x} + 2d_1k_2p_{3y}p_{5y} \\
&- 2L_{01}k_1p_{2x}p_{6x})x_2 - d_1k_2(L_3p_{3y} - p_{3x}p_{5y} + p_{5x}p_{3y}) \\
G_1 =&(L_3 + p_{2x} + p_{6x})^2x_2^2 + (L_3 + p_{2x} - p_{6x})^2 \\
G_2 =&(8L_3p_{6x})x_2 \\
G_3 =&(p_{2x} - L_3 + p_{6x})^2x_2^2 + (L_3 - p_{2x} + p_{6x})^2
\end{aligned}
$$

C Coefficient Definitions for Equations (16a)-(16d)

$$
\begin{aligned}
L_1 =&- L_3d_1k_2(p_{3y} + p_{5y})(L_{02} - d_2)x_2^2 - L_3(2d_1d_2k_1p_{6x} + \\
&2d_1d_2k_2p_{5x} - 2L_{01}d_2k_1p_{6x} - 2L_{02}d_1k_2p_{5x})x_2 - \\
&L_3d_1k_2(L_{02} - d_2)(p_{3y} - p_{5y}) \\
L_2 =&L_3(2d_1d_2k_1p_{2x} + 2d_1d_2k_2p_{3x} + 2d_1d_2k_1p_{6x} + 2d_1d_2k_2p_{5x} - \\
&2L_{01}d_2k_1p_{2x} - 2L_{02}d_1k_2p_{3x} - 2L_{01}d_2k_1p_{6x} - 2L_{02}d_1k_2p_{5x})x_2^2 - \\
&4L_3d_1k_2p_{5y}(L_{02} - d_2)x_2 + L_3(2d_1d_2k_1p_{2x} + 2d_1d_2k_2p_{3x} - \\
&2d_1d_2k_1p_{6x} - 2d_1d_2k_2p_{5x} - 2L_{01}d_2k_1p_{2x} - 2L_{02}d_1k_2p_{3x} + \\
&2L_{01}d_2k_1p_{6x} + 2L_{02}d_1k_2p_{5x}) \\
L_3 =&L_3d_1k_2(p_{3y} + p_{5y})(L_{02} - d_2)x_2^2 + L_3(2d_1d_2k_1p_{6x} + \\
&2d_1d_2k_2p_{5x} - 2L_{01}d_2k_1p_{6x} - 2L_{02}d_1k_2p_{5x})x_2 + \\
&L_3d_1k_2(L_{02} - d_2)(p_{3y} - p_{5y})
\end{aligned}
$$

$$
\begin{aligned}
M_1 =& - d_1k_2(L_{02}-d_2)(L_3p_{3y}-p_{3x}p_{5y}+p_{5x}p_{3y})x_2^2+\\
&(2d_1d_2k_1p_{2x}p_{6x}-2L_{02}d_1k_2p_{3x}p_{5x}-2L_{02}d_1k_2p_{3y}p_{5y}-\\
&2L_{01}d_2k_1p_{2x}p_{6x}+2d_1d_2k_2p_{3x}p_{5x}+2d_1d_2k_2p_{3y}p_{5y})x_2-\\
&d_1k_2(L_{02}-d_2)(L_3p_{3y}+p_{3x}p_{5y}-p_{5x}p_{3y})\\
M_2 =&2L_3(x_2^2+1)(d_1d_2k_1p_{2x}+d_1d_2k_2p_{3x}-\\
&L_{01}d_2k_1p_{2x}-L_{02}d_1k_2p_{3x})\\
M_3 =&d_1k_2(L_{02}-d_2)(L_3p_{3y}+p_{3x}p_{5y}-p_{5x}p_{3y})x_2^2+\\
&(2d_1d_2k_1p_{2x}p_{6x}-2L_{02}d_1k_2p_{3x}p_{5x}-2L_{02}d_1k_2p_{3y}p_{5y}-\\
&2L_{01}d_2k_1p_{2x}p_{6x}+2d_1d_2k_2p_{3x}p_{5x}+2d_1d_2k_2p_{3y}p_{5y})x_2+\\
&d_1k_2(L_{02}-d_2)(L_3p_{3y}-p_{3x}p_{5y}+p_{5x}p_{3y})\\
N_i =&G_i \quad \forall i=1,2,3
\end{aligned}
$$

$$
\begin{aligned}
O_1 =&(L_3^2+2L_3p_{3x}+2L_3p_{5x}+p_{3x}^2+2p_{3x}p_{5x}+p_{5x}^2+p_{3y}^2+\\
&2p_{3y}p_{5y}+p_{5y}^2)x_2^2+(4L_3p_{5y}+4p_{3x}p_{5y}-4p_{5x}p_{3y})x_2+\\
&L_3^2+2L_3p_{3x}-2L_3p_{5x}+p_{3x}^2-2p_{3x}p_{5x}+p_{5x}^2+p_{3y}^2-\\
&2p_{3y}p_{5y}+p_{5y}^2\\
O_2 =&(-4L_3p_{3y}-4L_3p_{5y})x_2^2+(8L_3p_{5x})x_2+4L_3p_{5y}-4L_3p_{3y}\\
O_3 =&(L_3^2-2L_3p_{3x}-2L_3p_{5x}+p_{3x}^2+2p_{3x}p_{5x}+p_{5x}^2+p_{3y}^2+\\
&2p_{3y}p_{5y}+p_{5y}^2)x_2^2+(4p_{3x}p_{5y}-4L_3p_{5y}-4p_{5x}p_{3y})x_2+\\
&L_3^2-2L_3p_{3x}+2L_3p_{5x}+p_{3x}^2-2p_{3x}p_{5x}+p_{5x}^2+p_{3y}^2-\\
&2p_{3y}p_{5y}+p_{5y}^2
\end{aligned}
$$

References

[1] A. Pugh, *An introduction to tensegrity*. Univ of California Press, 1976.

[2] M. Shibata, F. Saijyo, and S. Hirai, "Crawling by body deformation of tensegrity structure robots," in *2009 IEEE International Conference on Robotics and Automation*, pp. 4375–4380, May 2009.

[3] A. Iscen, A. Agogino, V. SunSpiral, and K. Tumer, "Flop and roll: learning robust goal-directed locomotion for a tensegrity robot," in *IEEE/RSJ International Conference on Intelligent Robots and Systems*, pp. 2236–2243, Sept. 2014.

[4] G. Tibert, *Deployable tensegrity structures for space applications*. PhD Thesis, KTH Royal Institute of Technology, Sweden, 2002.

[5] N. Veuve, S. Dalil Safaei, and I. F. C. Smith, "Active control for mid-span connection of a deployable tensegrity footbridge," *Engineering Structures*, vol. 112, pp. 245–255, Apr. 2016.

[6] D. E. Ingber, "The architecture of life," *Scientific American*, vol. 278, no. 1, pp. 48–57, 1998.

[7] S. M. Levin, "The tensegrity-truss as a model for spine mechanics: biotensegrity," *Journal of mechanics in medicine and biology*, vol. 2, no. 03n04, pp. 375–388, 2002.

[8] T. Liedl, B. Hgberg, J. Tytell, D. E. Ingber, and W. M. Shih, "Self-assembly of three-dimensional prestressed tensegrity structures from DNA," *Nature Nanotechnology*, vol. 5, pp. 520–524, July 2010.

[9] C. Sultan and R. T. Skelton, "Tendon control deployment of tensegrity structures," in *Smart Structures and Materials 1998: Mathematics and Control in Smart Structures*, vol. 3323, pp. 455–467, International Society for Optics and Photonics, 1998.

[10] S. H. Juan and J. M. Mirats Tur, "Tensegrity frameworks: static analysis review," *Mechanism and Machine Theory*, vol. 43, pp. 859–881, July 2008.

[11] J. Y. Zhang and M. Ohsaki, "Stability conditions for tensegrity structures," *International Journal of Solids and Structures*, vol. 44, pp. 3875–3886, June 2007.

[12] H. Murakami, "Static and dynamic analyses of tensegrity structures. Part 1. Nonlinear equations of motion," *International Journal of Solids and Structures*, vol. 38, pp. 3599–3613, May 2001.

[13] R. Connelly and W. Whiteley, "Second-order rigidity and prestress stability for tensegrity frameworks," *SIAM Journal on Discrete Mathematics*, vol. 9, pp. 453–491, Aug. 1996.

[14] M. Arsenault and C. M. Gosselin, "Kinematic, static and dynamic analysis of a planar 2-dof tensegrity mechanism," *Mechanism and Machine Theory*, vol. 41, pp. 1072–1089, Sept. 2006.

[15] C. Sultan, M. Corless, and R. E. Skelton, "The prestressability problem of tensegrity structures: some analytical solutions," *International Journal of Solids and Structures*, vol. 38, pp. 5223–5252, July 2001.

[16] S. Pellegrino, "Analysis of prestressed mechanisms," *International Journal of Solids and Structures*, vol. 26, pp. 1329–1350, Jan. 1990.

[17] R. E. Vasquez and J. C. Correa, "Kinematics, dynamics and control of a planar 3-DOF tensegrity robot manipulator," in *ASME 2007 International Design Engineering Technical Conferences and Computers and Information in Engineering Conference*, pp. 855–866, American Society of Mechanical Engineers, 2007.

[18] R. E. Vasquez, C. D. Crane, and J. C. Correa, "Analysis of a planar tensegrity mechanism for ocean wave energy harvesting," *Journal of Mechanisms and Robotics*, vol. 6, pp. 031015–031015–12, June 2014.

[19] A. A. T. M. Delissen, G. Radaelli, and J. L. Herder, "Design and optimization of a general planar zero free length spring," *Mechanism and Machine Theory*, vol. 117, pp. 56–77, Nov. 2017.

[20] J. L. Herder, *Energy-free Systems. Theory, conception and design of statically*, vol. 2. 2001.

[21] S. R. Deepak and G. K. Ananthasuresh, "Perfect Static Balance of Linkages by Addition of Springs But Not Auxiliary Bodies," *Journal of Mechanisms and Robotics*, vol. 4, pp. 021014–021014–12, Apr. 2012.

[22] D. Kapur, "Algorithmic elimination methods," in *Tutorial Notes, Intl. Symp. on Symbolic and Algebraic Computation (ISSAC), Montreal*, 1995.

[23] J. J. Sylvester, "On a theory of the syzygetic relations of two rational integral functions, comprising an application to the theory of sturm's functions, and that of the greatest algebraical common measure," *Philosophical Transactions of the Royal Society of London*, vol. 143, pp. 407–548, 1853.

[24] D. J. Bates, J. D. Hauenstein, A. J. Sommese, and C. W. Wampler, *Bertini: Software for numerical algebraic geometry*. 2006.